Supplementary material for *"Bare earth" structure-from-motion data: Evaluating color-based point classification and fine-scale topography*

R. Sare[1] and G. E. Hilley[1]

[1]Department of Geological Sciences, Stanford University, Stanford, CA, USA.

Corresponding author: Robert Sare (rmsare@stanford.edu)

Contents

Text S1. This supplement contains two tables of ground control and checkpoint locations. The vertical translation applied to each GCP for registration to the lidar ground surface is recorded in Table S1. The vertical differences between checkpoints and lidar and SFM point clouds are reported in Table S2. Table S3 gives the default parameters for the RBF-SVM classifier.

Figures S1-S4 show filtering results for site NW and BP as in the text. Figures S5 and S6 show the vertical differences at the checkpoints for the original checkpoint positions and registered checkpoints as summarized in Table 1. Figure S7 shows the location of the random lidar ground validation points used in Table 1.

In addition to the point-to-point comparison discussed in the text (Sections 2.3 and 4.2; Table 1), local cloud-to-cloud differences were also examined (Figure S8). The Multiscale Model to Model Cloud Comparison (M3C2) algorithm was used to measure cloud-to-cloud differences over the entire survey area (Lague et al., 2013; James et al., 2017). This method computes the local normal vectors of a set of core points in the source cloud. Using this direction, a search neighborhood is projected onto the target cloud. The average position of each cloud is calculated in its respective neighborhood and the M3C2 distance is the distance between these positions. For this analysis, we use a search radius of 11.75 m for both neighborhoods. This was applied to every point in a ground-classified SFM point cloud as core points and the vendor ground points as target points. The result is a local cloud-to-cloud difference at each SFM point

(Figured S8b). The spatial distribution of M3C2 differences is similar to the vertical differences after registration at the checkpoints (Figure S6) and lidar validation points (Figure S7).

To provide context for the accumulation analysis in the text, Figure S9 shows the distribution of partial accumulation areas derived from the lidar and SFM DEMs and area difference for every pixel exceeding 30 m^2. The plan form of each network is similar, with no major flow paths missing in the SFM date (Figure S9a, b). However, several missing junctions and differences in tributary flow contribute to large area differences in the larger channels (Figure S9c), similar to the result in Figure 7.

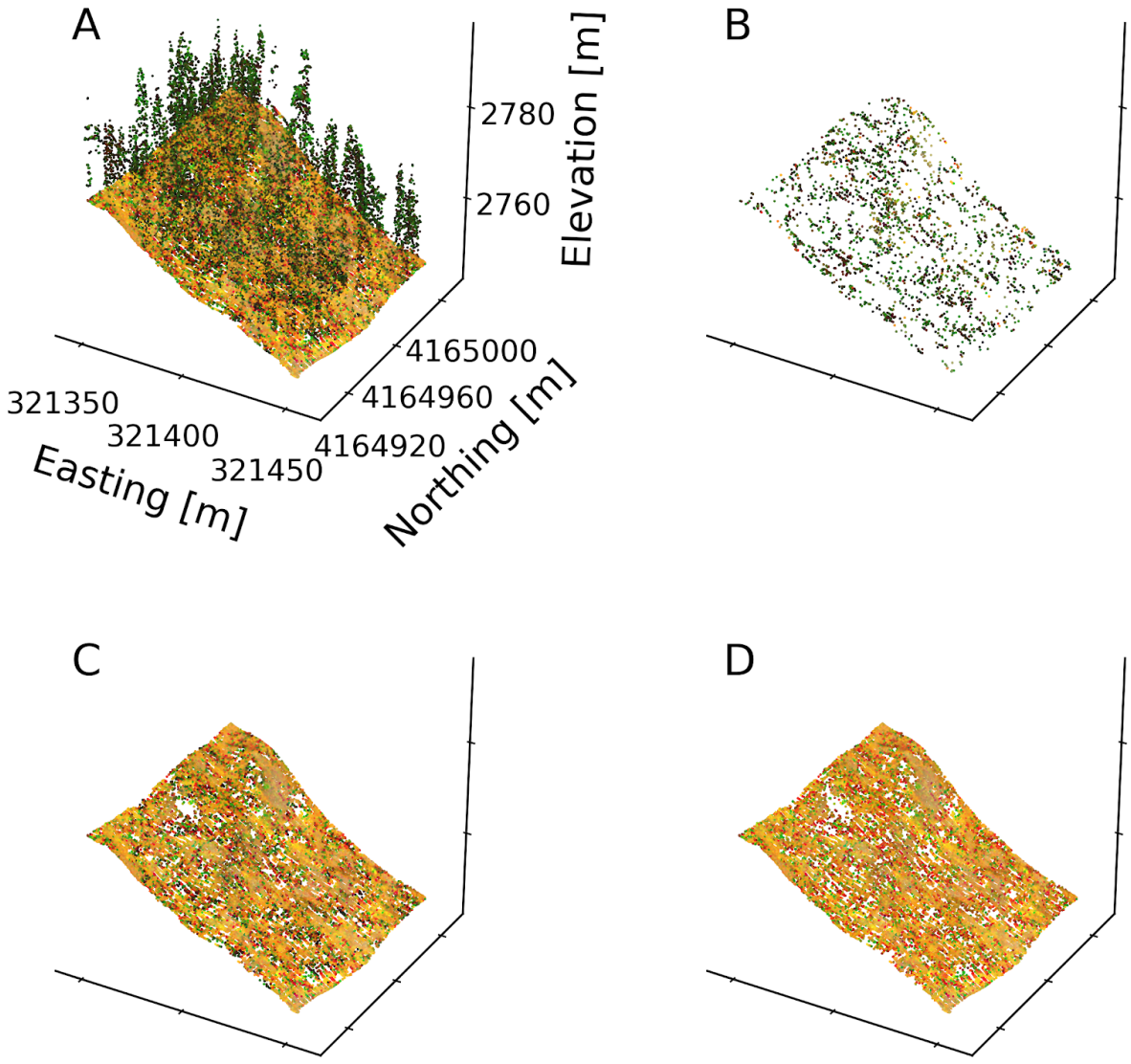

Figure S1. Results from lidar data at site NW: Horseshoe Lake tree kill. a) Full point cloud, b) Ground points that are reclassified by MCC-RGB, c) MCC ground points, d) MCC-RGB ground points.

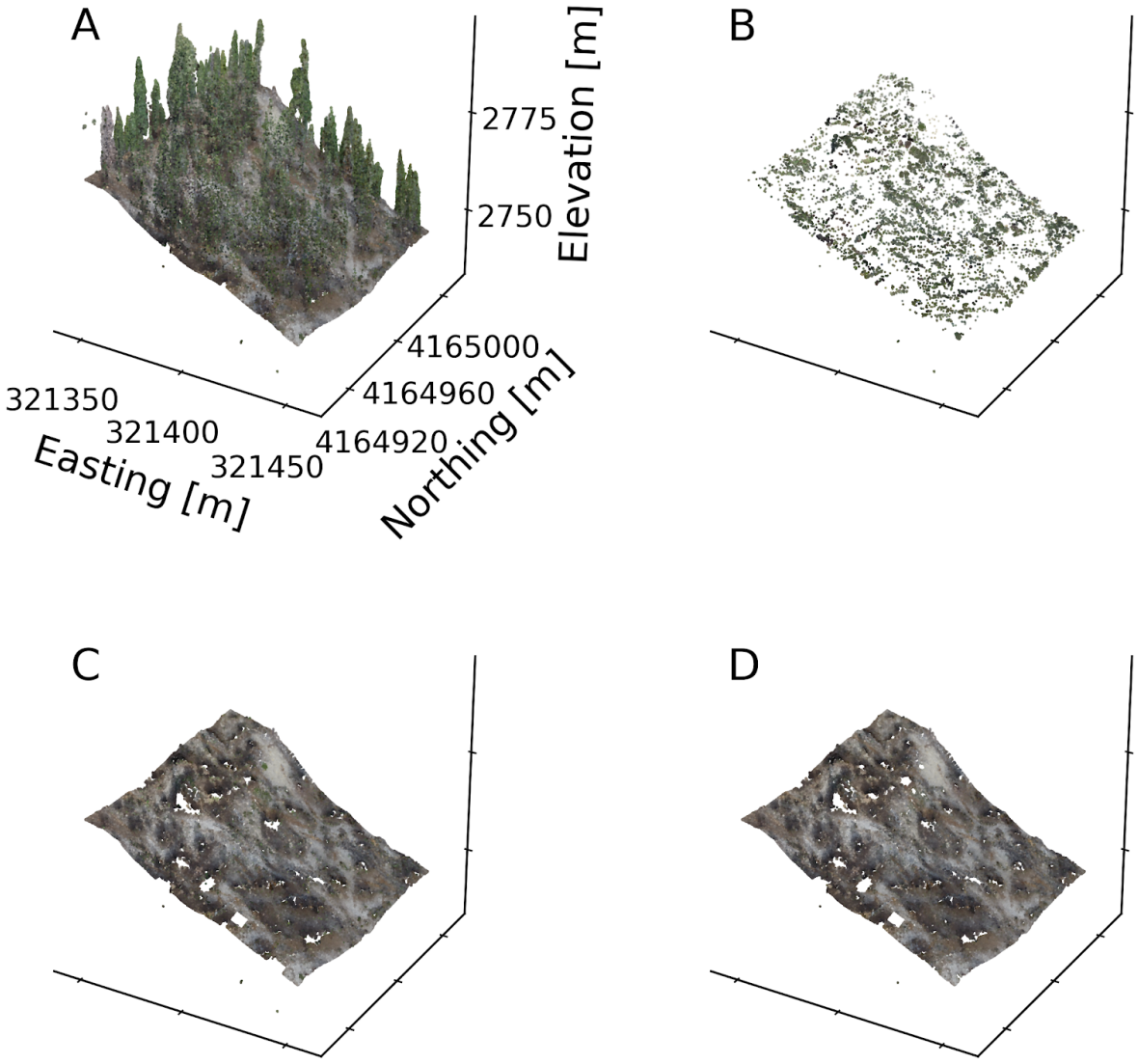

Figure S2. Results from SFM data at site NW: Horseshoe Lake tree kill. a) Full point cloud, b) Ground points that are reclassified by MCC-RGB, c) MCC ground points, d) MCC-RGB ground points.

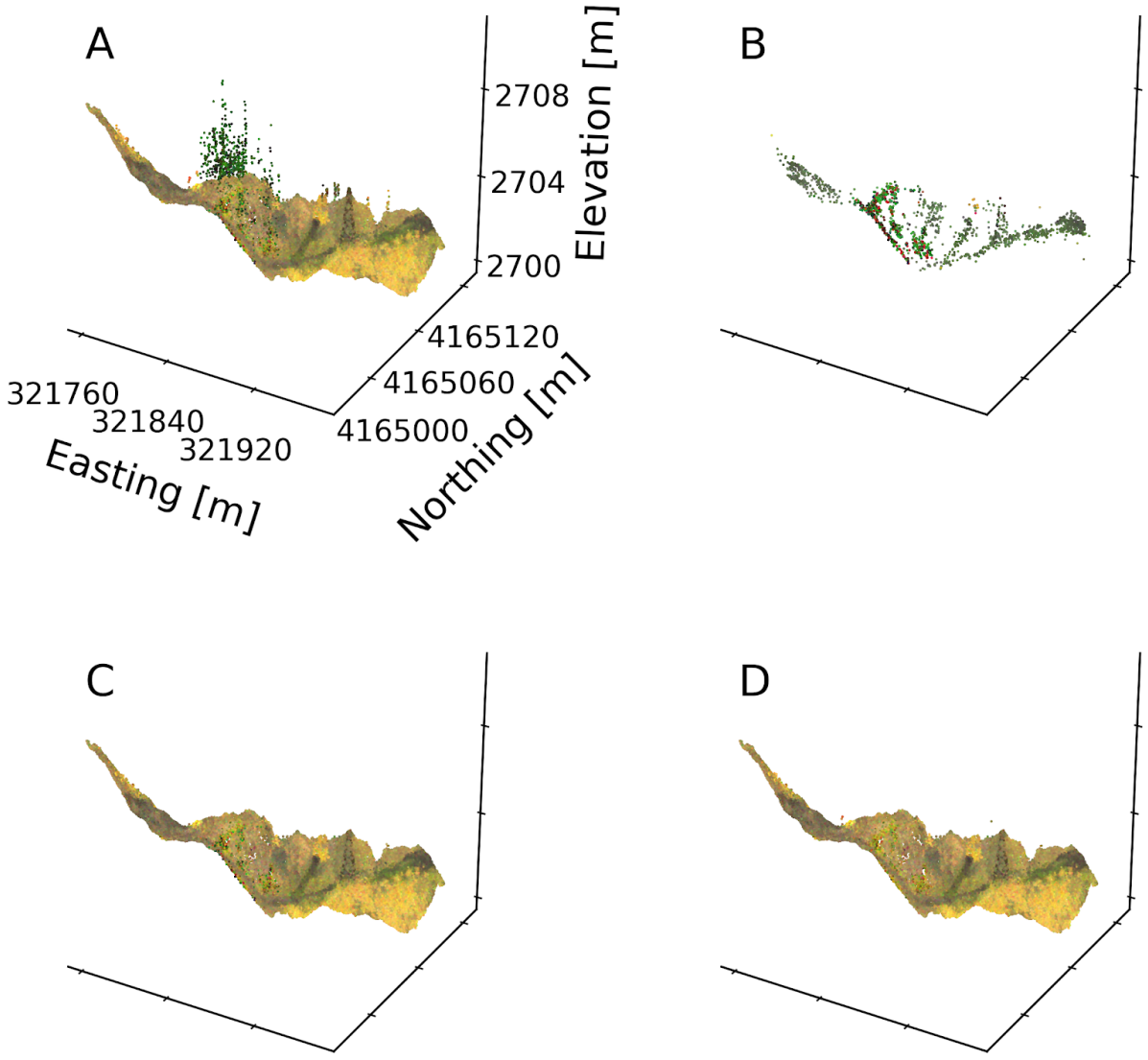

60

Figure S3. Results from lidar data at test site BP. a) Full point cloud, b) Ground points that are reclassified by MCC-RGB, c) MCC ground points, d) MCC-RGB ground points.

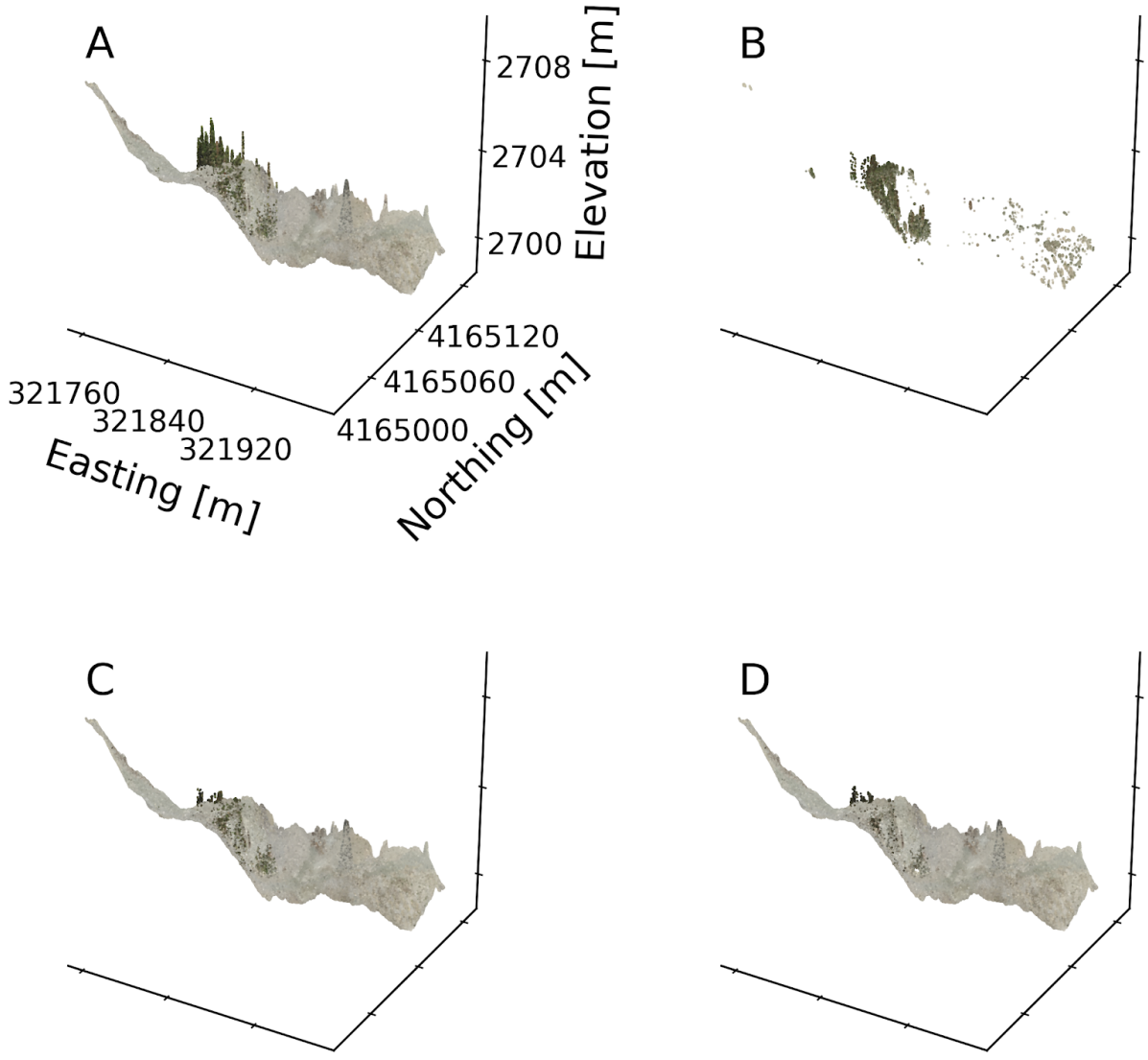

Figure S4. Results from SFM data at test site BP. a) Full point cloud, b) Ground points that are reclassified by MCC-RGB, c) MCC ground points, d) MCC-RGB ground points.

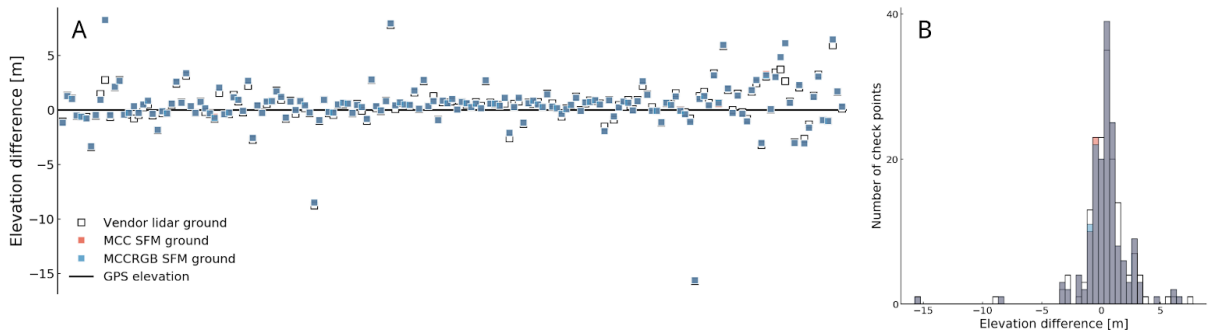

Figure S5. Check point vertical errors. a) Vertical difference between surveyed checkpoint elevations and vendor lidar ground classification (white), MCC ground classification (red), and MCCRGB ground classification (blue) of SFM data. Points are arbitrarily sorted from low to high elevation. b) Histogram of vertical differences in panel a. Red and blue squares correspond to differences mapped in Figure S6c and d.

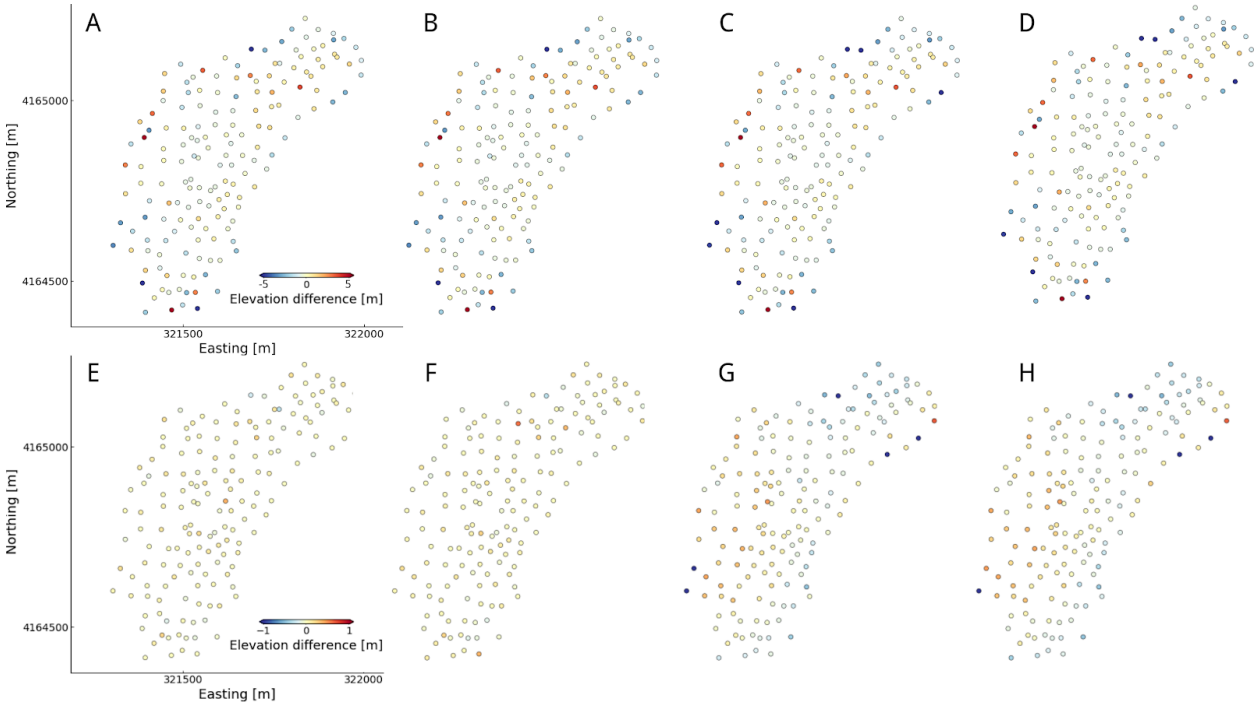

Figure S6. Vertical errors before (top row) and after registration (bottom row). a - d) Check point vertical errors against ground points from a) MCC applied to lidar, b) MCCRGB applied to lidar, c) MCC applied to SFM, d) MCCRGB applied to SFM. e) - h) Vertical differences between ground surface and checkpoints after registration to lidar elevations for e) MCC applied to lidar, f) MCCRGB applied to lidar, g) MCC applied to SFM, h) MCCRGB applied to SFM. Negative values indicate the test point is below vendor ground point. See Figure 3 for checkpoint network. Summary statistics given in Table 1.

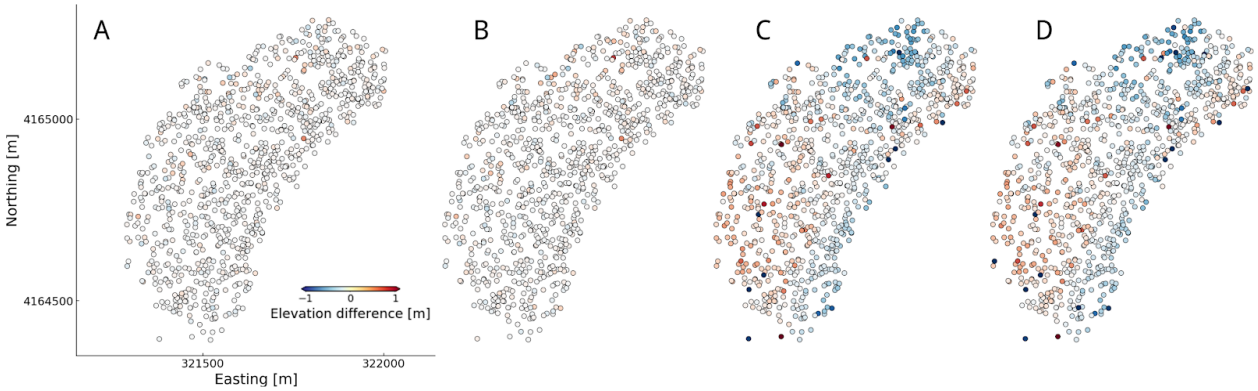

Figure S7. Randomly selected vendor ground lidar validation points used. a) MCC applied to lidar, b) MCCRGB applied to lidar, c) MCC applied to SFM, d) MCCRGB applied to SFM. Negative values indicate test point is below vendor ground point. These locations have a minimum point density of 10 points m^{-2} in the SFM point cloud as measured in a circular window of 1 meter radius. Summary statistics given in Table 1.

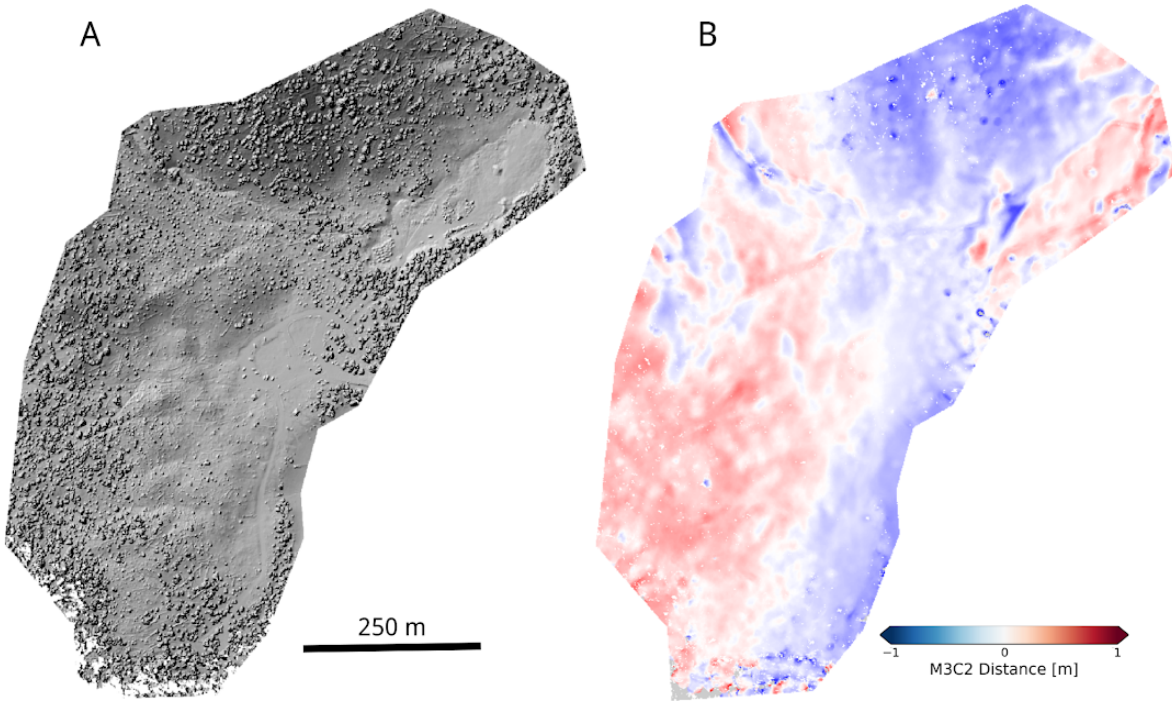

Figure S8. a) Hillshade produced from DEM using all structure-from-motion points, b) M3C2 distance between vendor ground points and SFM MCCRGB ground points. Search radius 11.75 m. See text for details.

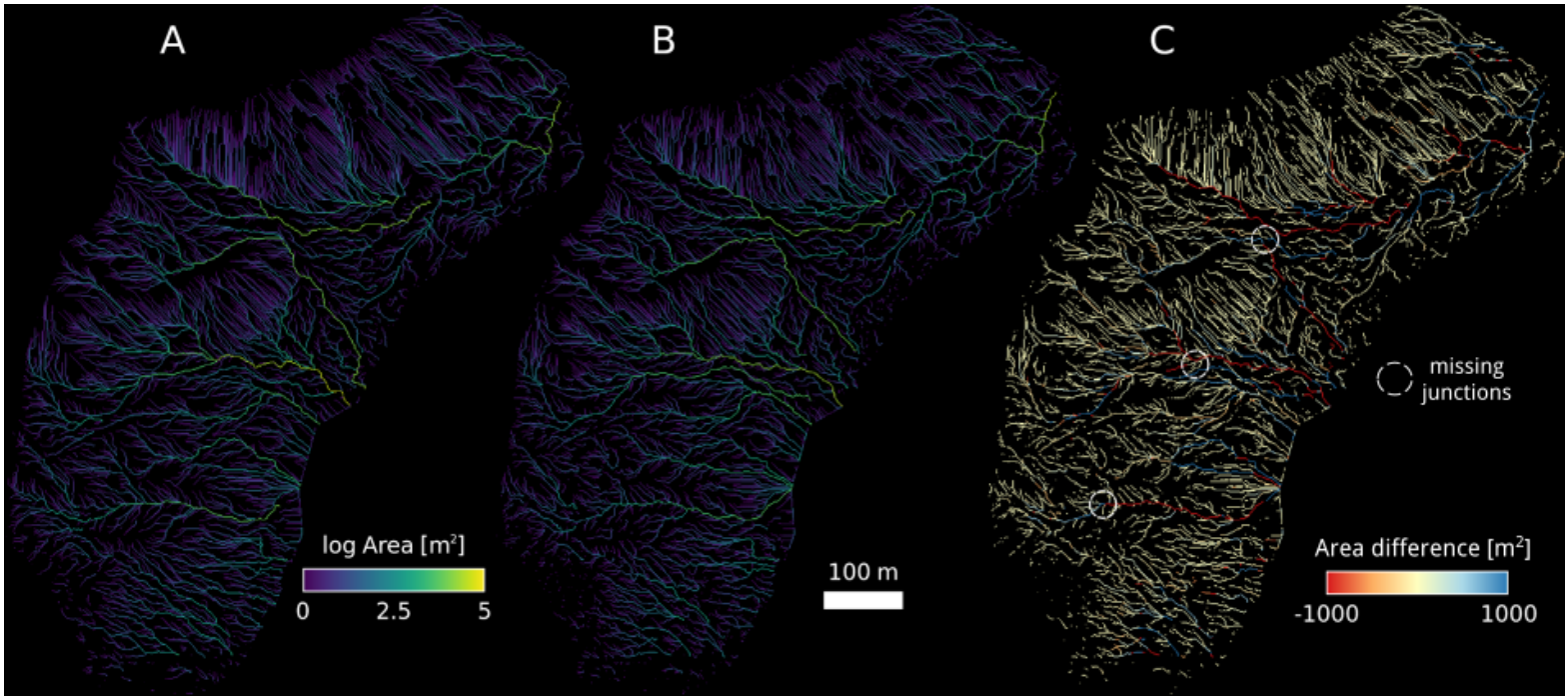

Figure S9. Partial accumulation area calculated using a) vendor bare earth DEM and b) SFM MCCRGB ground-only DEM. c) Local difference between areas (lidar - SFM) with major junctions not present in SFM-derived channel network (white circles). 1 m resolution. See text for details. Survey area outlined in Figure 2b.

Table S1. Ground control points used in UAV survey of HSL.

Table S2. Check points surveyed at HSL.

Table S3. Default parameters chosen for classification.